Newport Beach, CA, USA
ACTIVE 95
1995 July 06–08

ACTIVE CONTROL OF NOISE IN MAGNETIC RESONANCE IMAGING

Frederic G. Pla[1], Scott D. Sommerfeldt[2], Robert A. Hedeen[1]

1. General Electric Corporate Research & Development, Schenectady, NY 12301
2. Graduate Program in Acoustics, The Pennsylvania State University, State College, PA 16804

INTRODUCTION

Noise during a Magnetic Resonance Imaging (MRI) procedure is often mentioned by patients as a reason for discomfort. As a result, a prototype Active Noise Control (ANC) system for reducing noise levels to the patient was designed and tested on a GE Signa MRI system. The MRI noise generation mechanism is similar to that of a loudspeaker. Several high-current scanning signals are simultaneously passed through coils located inside the very intense magnetic field. The resulting electromagnetic forces deform the coils, generating an acoustic signal.

The frequency and time history of the acoustic signal varies greatly with the scanning sequence used. When MRI systems were first introduced, scanning sequences (scans) had relatively slow repetition rates, resulting in the characteristic banging noise of early MRI systems. As a consequence of their impulsive nature, most of the noise generated by slow scans is broadband with peaks at the resonance frequencies of the mechanical and acoustical system. In addition, a long impulse response of the order of 100 ms is present due to the low structural and acoustic damping.

Recent advances in MRI technology have resulted in the introduction of faster scan sequences with much higher repetition rates. The noise generated by these fast scans is tonal in nature with the typical fundamental frequency (inverse of the repetition rate) above 100 Hz. As a result, most of the noise generated by fast scans is at the scan fundamental frequency and its harmonics. Faster scans are also typically louder than slower ones since the sound level generated is roughly proportional to the scan repetition rate.

Active noise control is an attractive solution to the MRI noise problem, especially for patient noise. However, the implementation of a high performance ANC system for MRI has several challenges unique to the MRI environment. In addition, understanding the MRI noise generation and propagation mechanisms is crucial to the implementation of a high performance ANC system. Several in-depth experimental and analytical studies of the noise generation and propagation mechanisms were performed before the architecture of the active noise control system was designed.

The prototype ANC system tested is shown in Figure 1. It consists of a dual-Digital Signal Processor (DSP) controller and a pair of non-magnetic noise canceling sources and error

microphones placed inside the magnet bore in the vicinity of the patient. The bandwidth of the ANC system was chosen to cover the noise bandwidth of the MRI system, from about 200 Hz to 1.2 kHz, and the controller and sources were designed accordingly. The controller features a fast adaptation rate and on-line system identification, required since the main MRI system acoustic transfer functions vary with time during each scanning procedure. In addition, the controller was designed to cancel both slow/impulsive and fast/tonal scans. The two low-profile, high-output speakers used as canceling sources are not visible to the patient and do not restrict his motion. These custom-made non-magnetic speakers are powered by piezoceramic actuators.

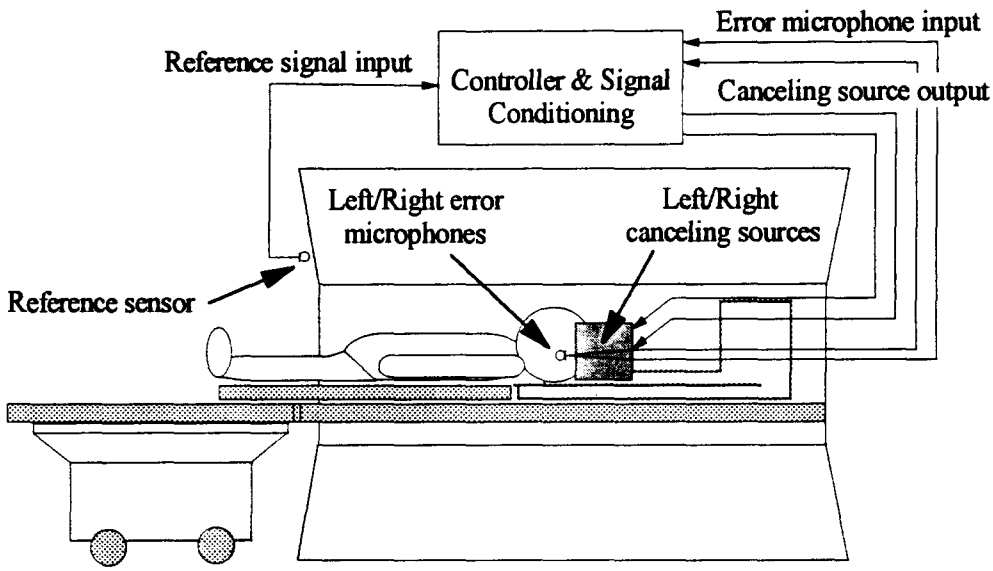

Figure 1 ANC system for MRI

DESIGN OF NON-MAGNETIC CANCELING SOURCES

The development of an appropriate canceling noise source suitable for use in the MRI environment presented a number of challenging constraints. First and foremost, the operation of the canceling system could not be allowed to affect the quality of the diagnostic images. This meant that neither ferrous metal nor (especially) magnetic fields could be allowed within about 10 meters of the scanner, precluding the use of conventional voice coil loudspeakers. (In any event, conventional speakers could not operate in the intense magnetic field of the scanner). Additionally, the canceling sources had to present a wide band response at a rather high level, with a reasonably short impulse response to simplify the system modeling. They had to be small and unobtrusive enough to be placed near the patient's ears in the narrow confines of the inner bore of the scanner, the use of headphones or other wearable equipment being deemed unsuitable for patient comfort.

We had early settled on a source employing a plastic diaphragm driven in a bending mode by a patch of piezoelectric material as presenting the best chance of meeting these design constraints. The issue became one of designing such a piezoelectric source with a suitable frequency response. We felt that a response that was reasonably flat from 200 Hz to 1.2 kHz would be suitable, being limited on the low end by the normal rolloff in the patient's hearing response and on the high end by the physical limitations of effective active noise cancellation.

After several iterations, we settled on a design similar to that shown schematically in Figure 2. Each source unit was a box of Lexan polycarbonate approximately 16 cm by 16 cm by 6 cm deep. The salient features of the canceling source include a 0.8 mm thick plate of Lexan polycarbonate, approximately 13 cm square, with a plate of Motorola PZT-5A piezoceramic bonded to the center as an actuator. The actuator plates were 0.4 mm thick and 66 mm square. The actuators were bonded with M&M GA-2 epoxy, which was chosen to present a stiffness similar to the Lexan diaphragm. The epoxy was carefully degassed to remove non-bonding air pockets and cured at elevated temperature. The piezoceramic actuators were employed in a 1-3 mode, in which the material dilates in a direction perpendicular to the direction of the imposed electric field. In this case, the field was imposed across the thickness of the material by thin electrical leads soldered to either side of the PZT.

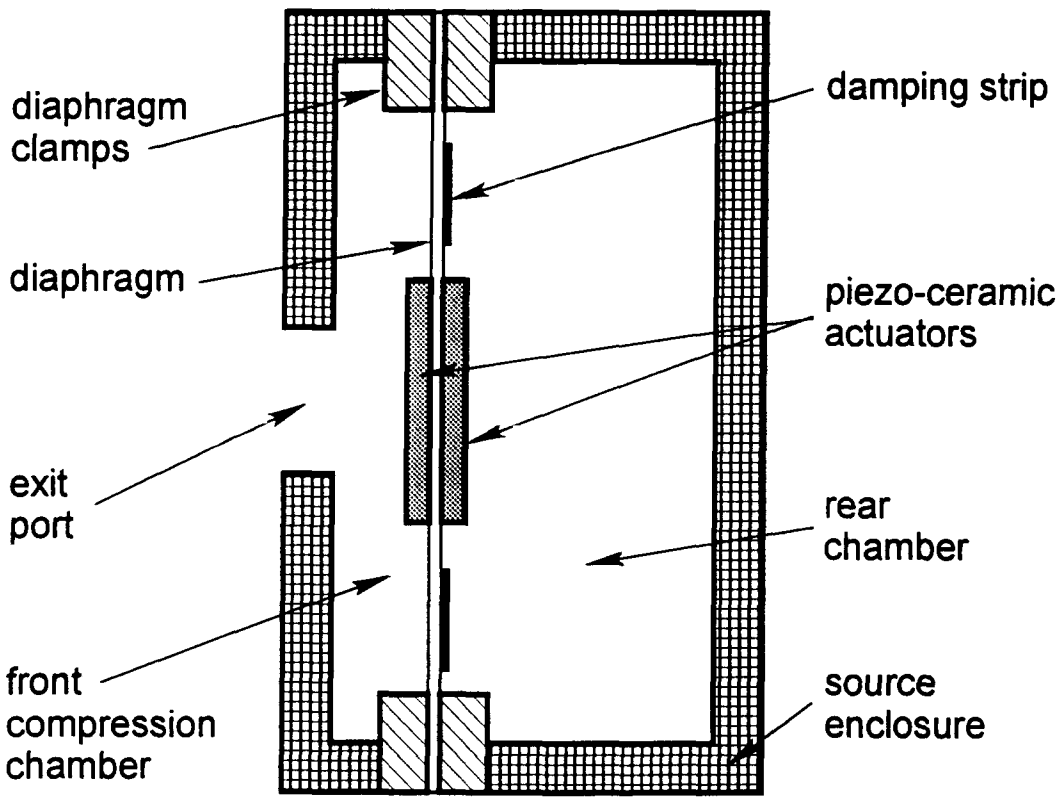

Figure 2 Schematic of canceling noise source

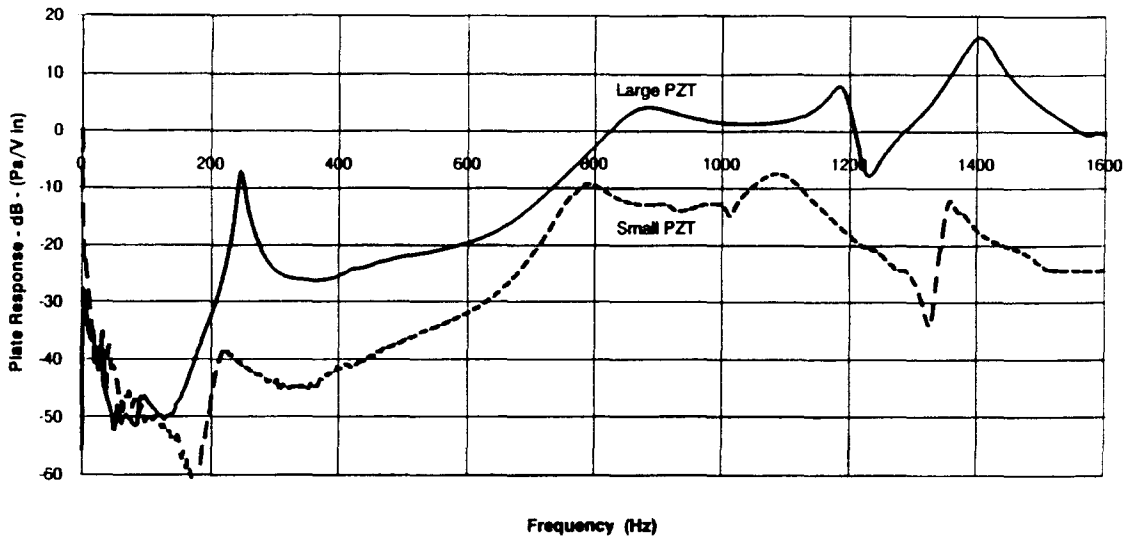

Figure 3 Gain Improvement using large actuators

Upon application of an electric field, the PZT expanded and contracted in the plane of the diaphragm. The periodic extension of the PZT actuators induced a couple acting out of the diaphragm plane, exciting the diaphragm in bending and producing motion normal to the diaphragm for efficient generation of sound. The magnitude of this couple, and hence the amplitude of resulting sound, was directly proportional to the size of the PZT actuators, as illustrated in Figure 3. We employed two PZT actuators, one on each side of the diaphragm and wired out of phase with each other, in order to double this applied couple.

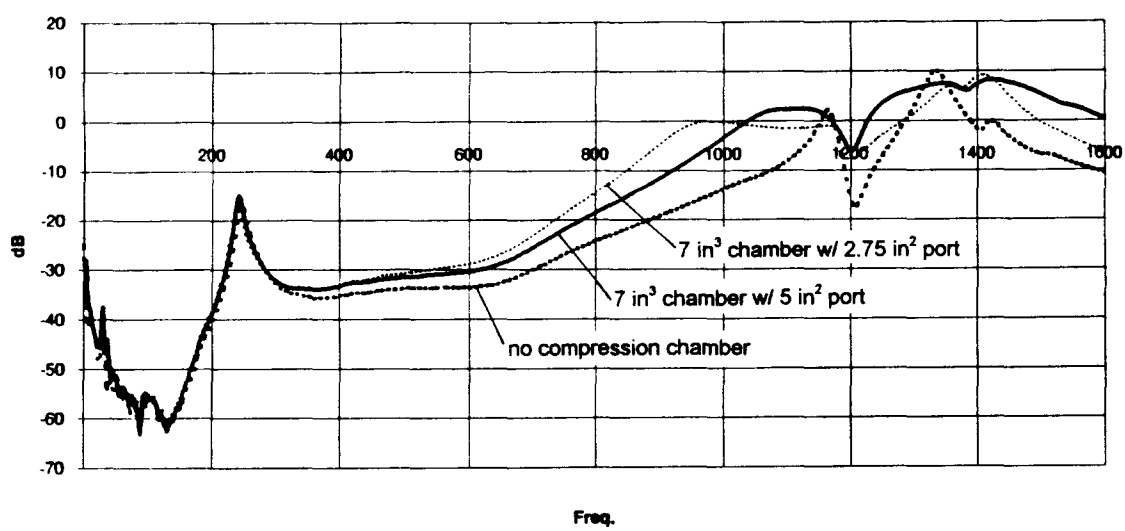

Figure 4 Response tuning with front chamber compression loading

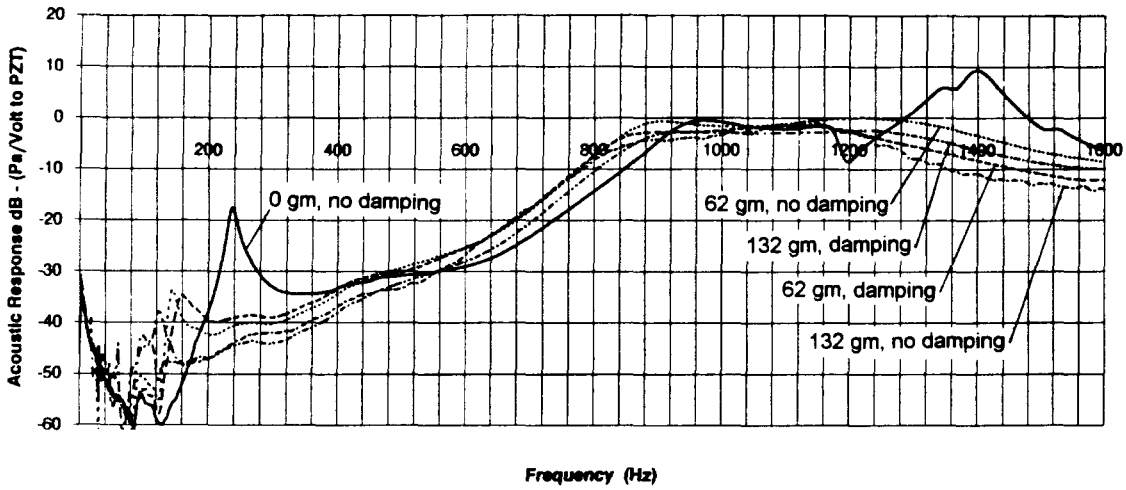

Figure 5 Response tuning by addition of mass and damping

The diaphragm was clamped in a rigid aluminum frame. We found that a clamped suspension gave a higher amplitude response than a compliant or simple support, with comparable resonant frequencies. The diaphragm was acoustically loaded by front and back pressure chambers. The back chamber volume was chosen to add appropriate low frequency compliance to the diaphragm suspension and the front chamber, fitted with a small port, was designed to adjust the acoustic impedance so as to maximize the sound power output. Figure 4 illustrates part of our process of tuning the output by adjusting the size of the port in the front cavity. The frequency response of the sources was further tuned by applying constrained layer damping and small discrete masses to the rear surface of the diaphragm. The damping consisted of a thin layer of compliant adhesive holding several strips of 0.4 mm thick polycarbonate. The damping and masses served to flatten the plate resonances of the diaphragm, especially the large response peak at about 240 Hz as may be seen in Figure 5.

The experimental work was augmented by finite element analysis of the predicted plate responses, and by lumped-parameter modeling using acoustic-electric analogs. In all, we managed by this process to increase the sound power output of our canceling sources by 45 dB over our initial design. We found that tuning of the front compression chamber and port had the greatest effect, followed by increasing the size and number of the PZT actuators. The sources were capable of producing sound pressure levels as high as 130 dB near the ports, with good transient response and a reasonably flat frequency response, which was more than adequate for canceling the loudest MR scan protocols.

CONTROLLER IMPLEMENTATION

For implementing active noise control in the MRI chamber, an adaptive feedforward control system was implemented. The controller was based on the multi-channel filtered-x

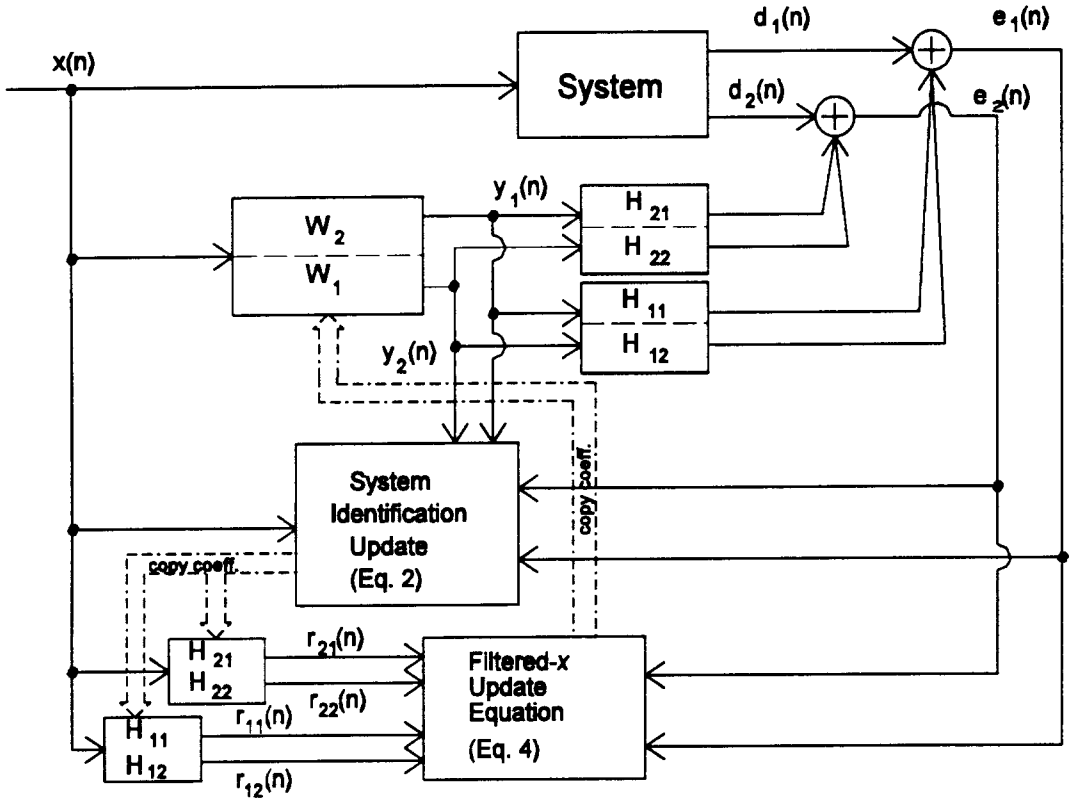

Figure 6 Block diagram of two channel system

algorithm, and was characterized by a single reference input, up to two control outputs, and up to two error sensors. Multiple MRI scans were tested. However, all of the scans exhibited a wide band response, with significant response throughout the frequency range up to 1.2 kHz. As a result, the algorithm was designed to operate as a broadband controller over the frequency range up to 1.2 kHz. This wide frequency range of operation dictated the use of a large number of filter coefficients during implementation, imposing a relatively high computational burden on the digital signal processing (DSP) board. To achieve the computational throughput required, the algorithm was implemented on a Spectrum Signal Processing DSP56001 Dual Processor Board. This DSP board features two 27 MHz Motorola DSP56001 DSP chips, which can be configured in a master/slave configuration to essentially double the computational capability from a single DSP chip.

The multi-channel algorithm incorporated both the filtered-x algorithm and on-line system identification. The system identification is necessary to develop a model of the transfer functions from the control output signals to the error input signals. These transfer functions are required to ensure proper convergence of the filtered-x algorithm. The method used for implementing the on-line system identification used only the information available from the control signals, the reference signal, and the error signals, and has been reported previously[1,2]. Other system identification approaches were tried initially, such as a fixed

broadband *a prior* identification, and the use of external random noise to identify the required transfer functions[3]. It was found that neither of these methods worked as well as the adaptive method using no additional external noise. This approach does require the modeling of two additional transfer functions from the reference input signal to the error signals. Thus, for a control system with two control actuators and two error sensors, there are a total of six system identification transfer functions that are adaptively modeled in real-time, in addition to the two adaptive control filters. To implement the system identification, an estimate of the measured error signals is determined using the reference input signal, $x(n)$, the control signals, $u_m(n)$, and the current transfer function estimates, C_l and H_{lm}. Here, H_{lm} represents the transfer function from the mth control signal to the lth error signal, and C_l represents the transfer function from the reference input signal to the lth error signal. The estimate of the lth measured error signal at discrete time n is then obtained as

$$\hat{e}_l(n) = \sum_{k=0}^{K-1} c_{lk}(n)x(n-k) + \sum_{m=1}^{2}\sum_{j=0}^{J-1} h_{lmj}(n)y_m(n-j); \qquad l=1,2 \tag{1}$$

where c_{lk} and h_{lmj} are the coefficients of the estimates of C_l and H_{lm}. The estimate of each transfer function is updated recursively according to

$$\begin{aligned} h_{lmj}(n+1) &= h_{lmj}(n) + \alpha u_m(n-j)[e_l(n) - \hat{e}_l(n)]; \qquad l,m=1,2 \\ c_{lk}(n+1) &= c_{lk}(n) + \alpha x(n-k)[e_l(n) - \hat{e}_l(n)]; \qquad l=1,2 \end{aligned} \tag{2}$$

where α is a convergence parameter chosen to maintain stability.

The transfer function estimates are used to calculate the filtered reference signals r_{lm}, required for implementation of the filtered-x algorithm. These filtered reference signals are obtained as

$$r_{lm}(n) = \sum_{j=0}^{J-1} h_{lmj}(n)x(n-j); \qquad l,m=1,2 \tag{3}$$

The filtered reference signals are then used to update the control filter coefficients w_{mi}, as

$$w_{mi}(n+1) = w_{mi}(n) - \mu\sum_{l=1}^{2} e_l(n)r_{lm}(n-i); \tag{4}$$

where μ is a convergence parameter chosen to maintain stability. Further details of the algorithm can be found in Reference 1, and a block diagram of the multi-channel control system implemented is shown in Figure 6.

RESULTS

Tests were performed over a period of several months using one of several MRI systems at the GE Corporate Research & Development Center in Schenectady, New York. Since these systems are used by the MRI group for internal research and development only, time and freedom were allowed to make structural and acoustic measurements, and to test various

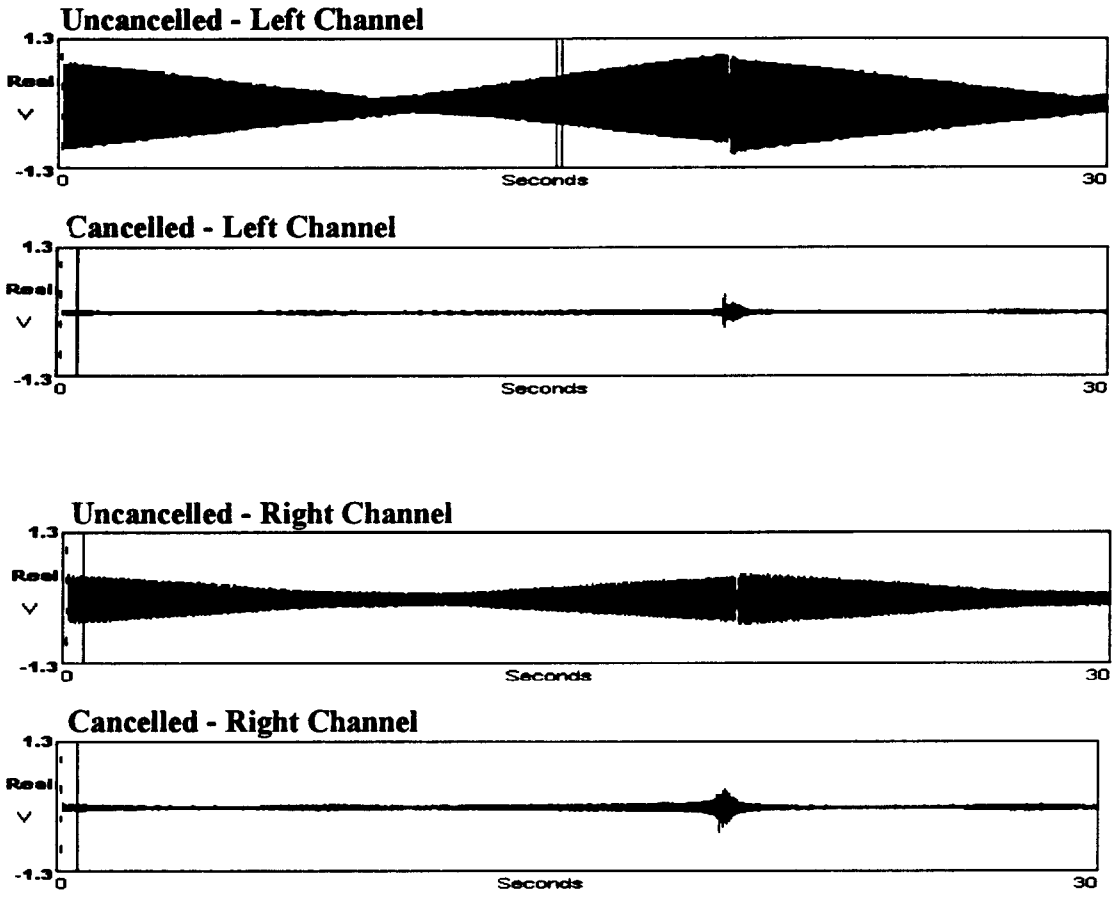

Figure 7 Time History - Left and right ear - Fast scan

system configurations which would not have been possible in a clinical environment.

The ANC system reduced the overall noise level at the patient by 15 dB to 25 dB for the noisiest scans. Some of the discrete frequencies were reduced by as much as 60 dB. The system was subjectively evaluated by several volunteers who underwent an MRI scan and who confirmed the large drop in noise. In addition, there was no observed degradation of image with the ANC system in operation.

Figure 7 shows a typical time history of the noise at each ear of the patient with the ANC system on and off. This particular test was performed with a fast scan at 100% power. The amplitude of the noise signal at the patient and its phase with respect to the reference signal

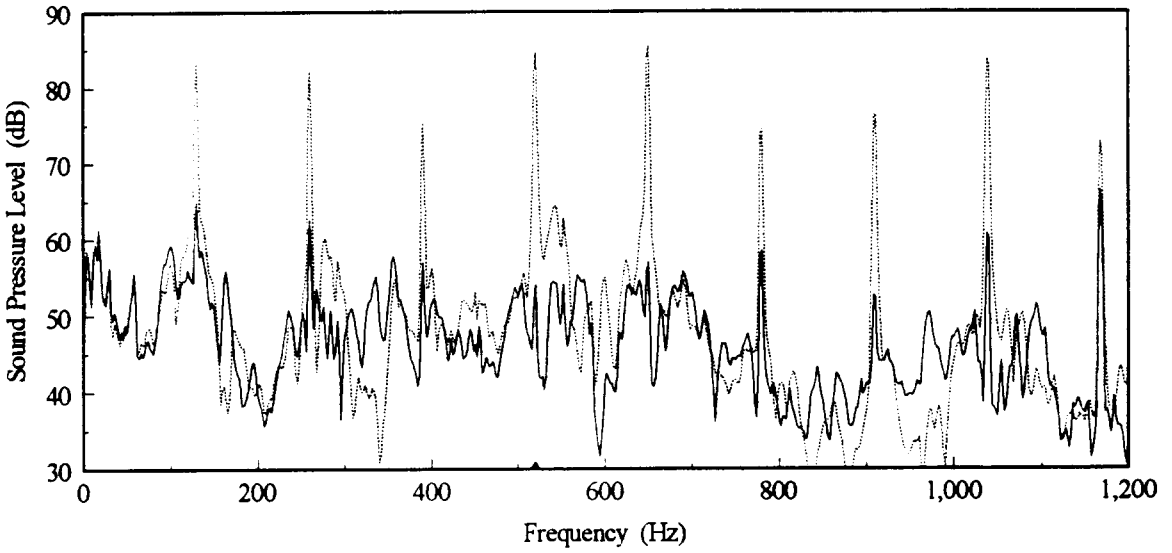

Figure 8 Frequency Spectrum - Left channel - Fast scan

vary with time as the individual axis scanning signals change in amplitude. The overall noise level averaged over a scan cycle dropped 18 dB at the left ear and 14 dB at the right ear when the ANC system was activated. The drop in noise level for the 0 to 1200 Hz bandwidth was 25 dB and 21 dB for the left and right ear respectively, showing the 6-7 dB contribution of the uncontrolled high frequencies to the residual noise. The maximum instantaneous noise reduction during the scan cycle was as high as 28 dB overall, and nearly 60 dB at some frequencies..

Figure 8 shows the frequency spectrum of the time signal in Figure 7. The spectrum was obtained by averaging the signal over several minutes. Noise is canceled from 130 Hz to 1.2 kHz by as much as 40 dB. Other tests were performed on slower impulsive scan sequences. Results showed a typical overall noise cancellation of about 10 dB, with peaks lowered by as much as 25 dB with a definite "whitening" of the spectrum. The subjective perception by volunteers was that of a much "thinner" sound with the characteristic hammering noise still perceivable.

Some of the residual noise when the ANC system is operating can also be attributed to uncanceled transients. Between each scan cycle, one or more of the scanning signals reverse phase, producing an abrupt change in the noise level. The effect of this phase change may be seen in Figure 7 where the system rings briefly while the controller adapts to the sudden change in the main MRI system transfer function. Excluding the transient, the overall noise reduction over the scan cycle is over 20 dB. This transient can be eliminated easily through software and hardware modifications to better tailor the controller architecture to the noise generation and propagation mechanisms. This however implies the use of a different controller

architecture for each major scan sequence for optimum performance, which was beyond the scope of this work.

CONCLUSIONS

An ANC system was successfully developed and tested on a GE Signa MRI system used for clinical imaging. The system consists of a dual-DSP controller with the following characteristics: 3 kHz sampling frequency, long impulse response, fast adaptation, and on-line system identification. A pair of high acoustic output, non-magnetic noise canceling sources inside the bore of the system provides the canceling acoustic signal. The custom-made canceling sources can generate sound pressure levels up to 130 dB several inches away from the patient from 200 Hz to 2 kHz and with good transient response.

The ANC system reduces the overall noise level at the patient by as much as 15 dB-25 dB for the noisiest scans. Discrete frequencies are reduced by as much as 60 dB, with test observers confirming the large drop in noise. For optimum performance, the noise generation and propagation mechanisms must first be identified in order to fit the controller architecture to the physical system. Substantial improvements in performance can be obtained by customizing the controller architecture to each class of scanning sequence to be canceled (such as slow scans or fast scans) and by increasing the controller frequency bandwidth.

REFERENCES

[1] "Multi-channel adaptive control of structural vibration," S. D. Sommerfeldt, *Noise Control Eng. J.* , **37**, 77-89 (1991).

[2] "Adaptive control of a two-stage vibration isolation mount," S. D. Sommerfeldt, J. Tichy, *J. Acoust. Soc. Am*, **88**, 938-944 (1990).

[3] "Development of the filtered-*U* algorithm for active noise control," L. J. Eriksson, *J. Acoust. Soc. Am.*, **89**, 257-265 (1991).